MODELING OF CRITICAL FLUX CONDITIONS IN CROSSFLOW MICROFILTRATION

Suhan Kim, and Heekyung Park

Department of Civil Engineering, Korea Advanced Institute of Science and Technology(KAIST), Taejon, Korea

Abstract: In the process of crossflow microfiltration, a deposit of cake layer tends to form on the membrane, which usually controls the performance of filtration. It is found, however, that there exists a condition under which no deposit of cake layer is made. This condition is called the sub-critical flux condition, and the critical flux here means a flux below which a decline of flux with time due to the deposit of cake layer does not occur. In order to study the characteristics of the critical flux, a numerical model is developed to predict the critical flux condition, and is verified with experimental results. For development of the model, the concept of effective particle diameter is introduced to find a representative size of various particles in relation to diffusive properties of particles. The model is found to be in good match with the experimental results. The findings from the use of the model include that the critical flux condition is determined by the effective particle diameter and the ratio of initial permeate flux to crossflow velocity.

Key Words: Crossflow Microfiltration, Critical Flux, Numerical Model, Effective Particle Diameter

1. INTRODUCTION

1.1 Critical flux in Microfiltration

Microfiltration (MF) is a pressure driven process using microporous membrane as a separating media. It is used to filter the suspensions containing colloidal or fine particles with linear dimensions in the range of 0.02 to 10μm. Most of the pollutants in water and wastewater fall in this size range and will be efficiently removed by MF. The MF process can be operated at either crossflow or deadend flow configuration. Crossflow microfiltration (CFMF) is advantageous over deadend flow configuration because in CFMF high shear tangential to membrane surface sweeps the deposited particles towards the filter exit(Belfort et al., 1994).

However, in practice, suspended particles are transported to the membrane surface by permeate flow due to the imposed pressure drop during CFMF, and a cake layer is formed by these particles. The cake layer formed on membrane surface induces membrane permeate flux decline. This is one

of the major problems in pressure-driven membrane processes. Over several decades, many studies about CFMF were carried out to overcome the flux decline problem. These studies mainly involved modifications of the membrane, the feed, and fluid dynamics in the membrane modules. The fluid dynamics approach focusses on the design of the membrane modules and optimization of the operating conditions. Especially for the microfiltration of particulate suspensions, efforts have mainly concentrated on modifying the fluid dynamics in membrane module (Kwon, 1998).

The concept of critical flux has been recently introduced with a number of experimental evidences. The concept of critical flux proposed by Field et al. (1995) and Howell (1995) states that "Critical flux is the flux below which a decline of flux with time does not occur and the value of critical flux depends on the hydrodynamics and probably also on the other variables." Operation below the critical flux is called sub-critical flux operation or clean non-fouling operation. If this operation can be sustained then the cost of cleaning are removed, energy is saved, and the only problem is that large areas of membrane must be used. This may not be a problem as increasingly we find that large scale operation of water treatment plants allows very large modules to be installed at very low unit costs for a square meter of membrane.

Field et al. (1995) and Howell (1995) proposed the concept of critical flux and carried out the study of critical flux by experimental data. Kwon (1998) studied about several factors affecting critical flux by experimental investigation. The methods of these studies have a tendency to depend on experimental investigation only. In this study therefore we approached the study of critical flux by mathematical modeling. Through modeling of three mass transfers (These are explained in next paragraph.) in CFMF, we are able to study in depth hydrodynamic factors affecting critical flux.

1.2 Three Mass Transfers in CFMF

In the membrane module of CFMF mass transfer can be well explained by Fig. 1. According to Fig. 1 mass transfer in membrane module is divided into convective mass transfer, backdiffusive mass transfer, and axial mass transfer. Convective mass transfer

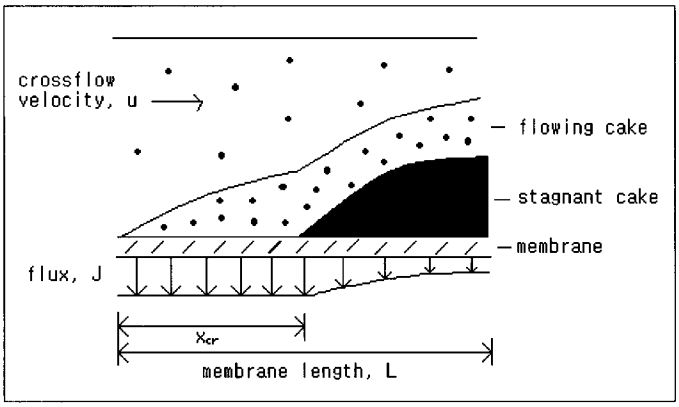

Fig. 1. Mass transfer of crossflow microfiltration

means that particles move from bulk suspension to membrane surface. Backdiffusive mass transfer is contrary to convective mass transfer. Axial mass transfer means that particles move with crossflow of bulk suspension. As flux J increases, convective mass transfer becomes dominant, and as diffusivity of particle increases, backdiffusive mass transfer becomes dominant. Axial mass transfer increases with crossflow velocity increase. The diffusivity of particle is expressed by diffusion coefficient which is given by Eq. 1(Lee, 1997).

$$D_{eff} = D_m + D_s = \frac{kT}{6\pi\mu a} + 0.03\gamma a^2 \qquad \gamma = \left| \frac{\partial u}{\partial r} \right| \tag{1}$$

Where, D_{eff} is the effective diffusion coefficient, D_m the molecular diffusion coefficient, D_s the shear-induced hydrodynamic diffuison coefficient, k the Boltzmann constant, T the absolute temperature, μ the viscosity, a the particle radius, u the velocity, r the coordinate perpendicular to the velocity and γ is the shear rate.

In the case of particle with size range over 0.1㎛, D_{eff} is approximately D_s, this means the diffusivity of particle with size rage over 0.1㎛ is proportional to shear rate. And shear rate is generally increased with crossflow velocity increase. Therefore backdiffusive mass transfer is dominant with crossflow velocity increase.

In steady state, the concentration in the membrane is constant because these three mass transfers are in equilibrium. When axial and backdiffusive mass transfer are dominant over convective mass transfer, the concentration near membrane surface is low. If the concentration near membrane surface is low enough to sustain initial flux, this filtration operation is named sub-critical flux operation. In Fig. 1 x_{cr} means the length where no particle deposition occurs and L means membrane length. It is said that the critical flux condition is established for filtration, when x_{cr} reaches L.

2. METHODS AND MATERIALS

2.1 Prediction of critical flux condtion

In this study, the numerical model is used to find sub-critical flux condition. Modeling procedure is divided into four steps as follows: (1) formulation of mass balance equation, (2) determination of velocity distribution in the membrane module, (3) finding concentration distribution in the membrane module as solution of mass balance equation, and (4) confirming that concentration distribution satisfies mass balance. Fig. 2 simplifies the membrane module and shows the problem domain of a two-dimensional numerical model.

The membrane module used for this study is tubular module with inner radius 0.8㎜. For tubular membrane module, mass balance equation is given by Eq. 2 (MA et al., 1985).

$$u\frac{\partial c}{\partial x} + \left(v - \frac{1}{r}D_r\right)\frac{\partial c}{\partial r} = D_r\frac{\partial^2 c}{\partial r^2} \tag{2}$$

Here, u is the x-direction velocity, v is the r-direction velocity, c is the concentration, and, D_r is the diffusion coefficient in r-direction. In Eq. 2 the first term of left side means the axial mass transfer, the second term means the convective mass transfer, and right side means the backdiffusive mass transfer. In order to develop a model several basic assumptions are needed. These assumptions are as follows:

(1) Crossflow of suspension is laminar and viscous.

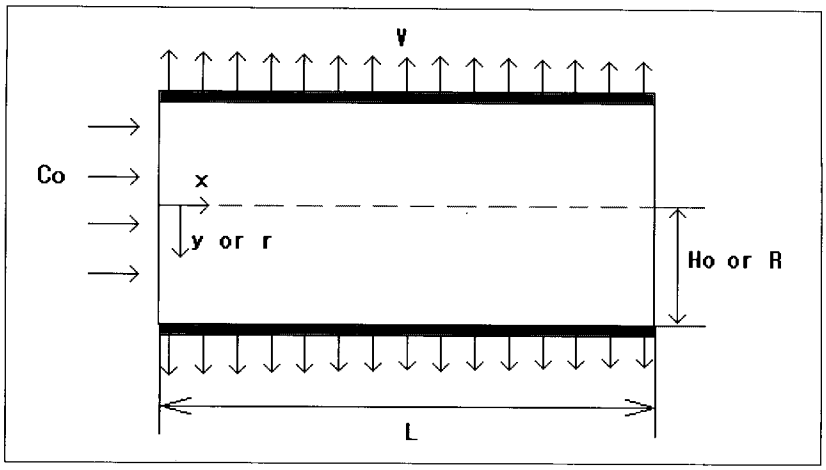

Fig. 2. Problem domain of two-dimensional numerical model

(2) In sub-critical flux condition velocity distribution is not different with initial distribution.

(3) Particles are sphere and their sizes are bigger than membrane pore size.

(4) Particles are lifted from the membrane surface by the shear-induced hydrodynamic diffusion and the surface charge has insignificant effect.

For a tubular membrane module, pressure and velocity distributions are expressed by Eq. 3a-3e (Brian, 1965); (Kleinstreuer et al., 1983); (Bouchard et al., 1994).

$$P(x) = P(0) - \frac{f_r u_{avg}(0)\mu x}{r^2} \tag{3a}$$

$$v_p(x) = \frac{P(x)}{\mu R_m} \tag{3b}$$

$$u_{avg}(x) = u_{avg}(0) - \frac{2}{R}\int_0^x v_p(x)dx \tag{3c}$$

$$u(x,r) = 2u_{avg}(x) - \left(1 - \left(\frac{r}{R}\right)^2\right) \tag{3d}$$

$$v(x,r) = v_p(x) - \left(2\left(\frac{r}{R}\right) - \left(\frac{r}{R}\right)^3\right) \tag{3e}$$

Where $P(x)$ is the transmembrane pressure distribution in x-direction, fr is the friction factor of membrane, $u_{avg}(x)$ is the average crossflow velocity distribution in x-direction, $v_p(x)$ is the permeate flux distribution, and R_m is the membrane resistance.

Concentration distribution in sub-critical flux condition is obtained by solving Eq. 2. Eq. 2, mass balance equation is solved by FDM (Finite Difference Method) after solving Eq. 1 (the diffusion coefficient), Eq. 3 (the velocity distributions).

Final procedure is the confirming that concentration distribution satisfies mass balance. If this concentration distribution satisfies mass balance, then particle size, crossflow velocity, and initial permeate flux at this time satisfy sub-critical flux condition. But if not, real velocity distribution differs from theoretical velocity distribution (Eq. 3) because of flux decline induced by particle deposition. So, we can recognize that this case does not satisfy critical flux condition. To check mass balance in a membrane module, we used the fact that particles do not penetrate membrane (assumption (3)) and Eq. 4. Assumption (3)

means vertical (perpendicular to membrane) mass balance and Eq. 4 means horizontal (parallel with membrane) mass balance.

$$\left(\int_0^r u \cdot cdA\right)_x - \left(\int_0^r u \cdot cdA\right)_{x+\Delta x} = 0 \qquad (4)$$

Additionally in order to check if laminar flow condition is satisfied (assumption(1)), Reynolds number(Re) is checked if it is over 2000 (for the case of pipe flow) or not. Among the sub-critical flux conditions searched by this procedure, the critical flux condition is determined as the highest flux condition where the other conditions are same.

2.2 The concept of effective particle diameter

For comparison of the experimental and modeling results, a representative value of particle size is needed because particles used in the experiment had various sizes while particle assumed in the model had a single size. This representative particle size is here called as "effective particle diameter". Effective particle diameter can be calculated using Eq. 6.

$$\text{Effective particle diameter} = \sum N_i w_i a_i \qquad (6a)$$

$$w_i \propto 1/D_i \propto 1/a_i^2 \text{ that is } w_i = k/a_i^2, \text{ k is constant} \qquad (6b)$$

$$\sum w_i N_i = k\sum(N_i/a_i^2) = 1 \text{ that is } k = 1/\sum(N_i/a_i^2) \qquad (6c)$$

Where, a_i is the diameter of each particle, N_i is the ratio of a particle whose size is a_i, and w_i is weighting factor which reflects the diffusivity of each particle. The larger the effect on concentration polarization is, the larger the weighting factor is. The smaller the diffusion coefficient is, the larger the effect on concentration polarization is. Therefore, weighted factor is inversely proportional to diffusion coefficient like Eq. 6b. Since diffusion coefficients of those particles whose sizes are over 0.1㎛ are approximately proportional to the square of

Table 1. Calculation of effective particle diameter for $CaCO_3$

Particle size range (㎛)	Average size per each size range, a_l (㎛)	Percentage of particle, N_i(%)	Weighted factor, w_l	$N_i w_i a_i$ (m)
1.53 - 2.0	1.765	5.45	9.725	0.935
2.02 - 3.0	2.51	4.51	4.809	0.544
3.09 - 3.9	3.495	2.33	2.48	0.202
3.98 - 5.0	4.49	5.00	1.5	0.337
5.01 - 6.9	5.955	5.06	0.854	0.257
6.99 - 9.6	8.295	5.89	0.44	0.215
9.69 - 15.0	12.345	11.12	0.199	0.273
15.0 - 20.4	17.7	14.38	0.0967	0.246
20.49 - 29.9	25.195	22.07	0.0477	0.265
29.9 - 40.1	35	12.57	0.0247	0.109
40.1 - 49.5	44.8	6.89	0.0151	0.047
49.5 - 74.1	61.8	3.56	0.0079	0.017
74.1 - 99.0	86.55	1.06	0.004	0.004
99.0 - 162.0	130.5	0.11	0.0018	0.003

Effective particle diameter = $N_i w_i a_i$ = 3.46㎛

particle diameter (Lee, 1997) and since particles used in this study have diameters over 0.1㎛, weighted factor is inversely proportional to the particle diameter. Using Eq. 6, the effective particle diameters of $CaCO_3$, kaolin, bentonite, bentonite(II), and $Mg(OH)_2$ are calculated to be 3.46㎛, 2.53㎛, 2.92㎛, 3.80㎛, and 2.85㎛. Table 1 shows an example of the calculation of effective particle diameter for $CaCO_3$.

As shown in table 1, smaller particles have larger weighted factor than larger particles. So, the effective particle diameter is nearly subjected to distributions of small particles whose sizes are several ㎛. Despite of mean diameter of 21.53㎛, the effective particle diameter of $CaCO_3$ is 3.46㎛. This large difference is induced by the distributions of small particles.

2.3 Experiments

In order to verify the use of the numerical model for prediction of the critical flux condition, experiments were conducted as described below. The schematic diagram of the microfiltration set-up used in this study was shown in Fig. 3. Suspensions dispersed by a stirrer were delivered from a feed tank to membrane by a variable speed tubing pump. For the suspensions, $CaCO_3$(mean particle diameter 21.53㎛), Kaolin(4.11㎛), bentonite (6.25㎛), bentonite(II)(47.23㎛) and $Mg(OH)_2$ (6.03㎛) were used and their concentration was 0.5g/L. Here bentonite(II) means bentonite sieved by 26㎛ sieve. Both the permeate and retentate lines were returned to the feed tank to maintain constant inlet condition and to check mass balance condition of the system. The pressure in membrane was controlled by two valves in permeate and retentate line and transmembrane pressure was obtained by Eq. 5.

$$P_{tm} = \frac{P_{in} + P_{out}}{2} \tag{5}$$

Where, P_{tm} is the transmembrane pressure, P_{in} the pressure of membrane inlet, and P_{out} the pressure of membrane outlet.

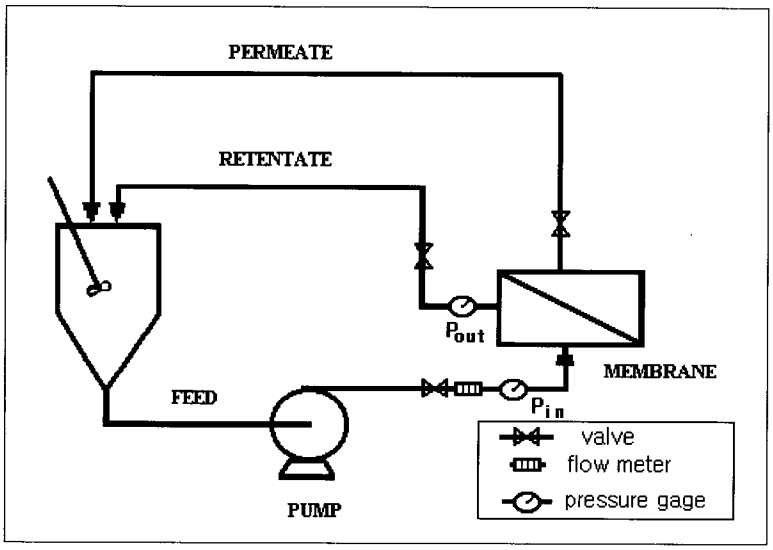

Fig. 3. The schematic of microfiltration system

3. RESULTS AND DISCUSSION

3.1 The effect of crossflow velocity on critical flux condition

Fig. 4 shows the effect of crossflow velocity on critical flux condition by comparing the experimental results of $CaCO_3$ with prediction results by the numerical model using effective particle diameter of $CaCO_3$. From the results shown in Fig. 4, we can draw the following conclusions :

(1) Since the modeling results are fairly close to the experimental results, we can say that the critical flux condition can be predicted by using the numerical model.

(2) The relationship of initial flux to crossflow velocity in the critical flux condition is found to be linear. Therefore, the critical flux condition can be described as the ratio of permeate flux(critical flux) to crossflow velocity.

3.2 The effect of particle size on critical flux condition

As discussed above, the critical flux condition is found to be described as the ratio

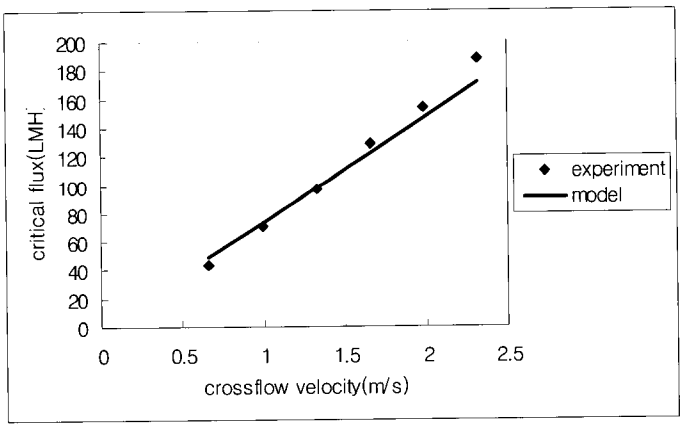

Fig. 4. The effect of crossflow velocity on critical flux condition in the case of $CaCO_3$

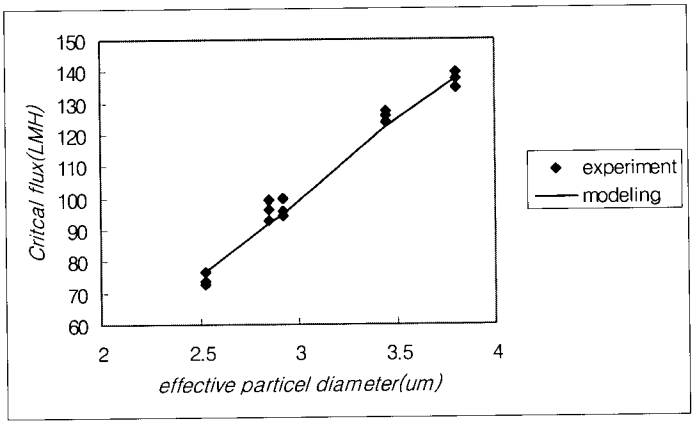

Fig. 5. The effect of particle size on critical flux condition (crossflow velocity = 1.65m/s)

of initial flux to crossflow velocity. Hydrodynamic factors effecting the critical flux condition are not only velocity distribution in the membrane module but also particle size. Therefore, the effect of particle size on the critical flux condition need to be studied in depth. Fig. 5 shows the effect of particle size on critical flux condition.

Fig. 5 describes the relationship between the critical flux condition and the effective particle diameter. As shown in Fig. 5, the larger effective particle diameter is, the larger critical flux is. Consequently, this result say that if the sizes of particles which consist of suspension become large, relatively large flux can be gained in the critical flux condition.

4. CONCLUSIONS

This study has constructed a modeling procedure for prediction of the critical flux condition. And, it also verified the modeling results with the experimental results to show their close match. The conclusions gained from this study are as follows:

(1) The numerical model developed in this study can predict the concentration distribution of particles in the membrane module under a certain operation condition which is subjected to the sub-critical flux condition. In the same way, it can also predict the critical flux condition.

(2) For comparison of the experimental and modeling results, it is found that a representative value of particle size is needed because particles used in the experiment have various sizes while particle assumed in the model has a single size.

(3) In the sub-critical flux condition, particle deposition on membrane surface does not occur since the concentration polarization effect is negligible. The critical flux condition is defined as the highest initial flux per crossflow velocity among the sub-critical flux conditions.

(4) The critical flux condition can be found at a relatively small ratio of initial flux to crossflow velocity. The larger the effective particle diameter is, the larger the initial flux per crossflow velocity is. Consequently, it can be said that the increase of particle size in suspension increases the permeate flux in the critical flux condition.

REFERENCE

Belfort G., Davis R. H. and Zydney A. L. (1994). *Review: The behavior of suspensions and macromolecular solution in crossflow microfiltration*, Journal of Membrane Science, Vol. 96, pp. 1-58

Bouchard C. R., Carreau P. J., Matsuura T., and Sourirjan S. (1994), *Modeling of ultrafiltration: prediction of concentration polarization effect*, Journal of Membrane Science, Vol. 97, pp. 215-229

Brian P. L. T. (1965), *Concentration polarization in reverse osmosis desalination with variable flux and incomplete salt rejection*, Ind. Eng. Chem. Fundam., Vol. 4, pp. 439-445

Field R. W., Wu D., Howell J. A. and Gupta B. B. (1995). *Critical flux concept for microfiltration fouling*, Journal of Membrane Science, Vol. 100, pp. 259-272

Howell J. A. (1995). *Sub-critical flux operation of microfiltration*, Journal of Membrane Science, Vol. 107, pp. 165-171

Kim S. (1999). *Prediction of critical flux conditions in crossflow microfiltration using a concentration polarization model*,

MS Thesis, Deptartment of Civil Engineering, Korea Advanced Institute of Science and Technology(in Korean)

Kleinstreuer C. and Paller M. S. (1983), *Laminar dilute suspension flows in plate-and-frame ultrafiltration units*, AIChE J., Vol. 29, No. 4, pp. 529-533

Kwon D.Y. (1998), *Experimental investigation on Critical flux in cross-flow microfiltration*, PhD Thesis, Faculty of Eng. Environmental Eng. Group, University of Technology, Sydney, Australia

Lee Y. and Clark M. M. (1997). *A numerical model of steady-state permeate flux during cross-flow ultrafiltration*, Desalination, Vol. 109, pp. 241-251

MA R. P., Gooding C. H. and Alexander W. K. (1985). *A dynamic model for low-pressure, hollow-fiber ultrafiltration*, AIChE J., Vol. 31, No. 10, pp. 1728-1732

Suhan Kim and Heekyung Park, Department of Civil Engineering, Korea Advanced Institute of Science and Technology(KAIST), Taejon, Korea

(e-mail: hans@kaist.ac.kr, hkpark@kaist.ac.kr)

(Received September 7, 1999; accepted March 23, 2000.)